

Inverse heat transfer problems: an application to bioheat transfer

Marek Rojczyk^{1,2}, Helcio R.B. Orlande¹, Marcelo J. Colaço¹,
Ireneusz Szczygieł², Andrzej J. Nowak², Ryszard A. Białeczki²,
Ziemowit Ostrowski²

¹ *Departament of Mechanical Engineering
Politécnica/COPPE, Federal University of Rio de Janeiro UFRJ
Cid. Universitária, Cx. Postal: 68503, Rio de Janeiro, RJ, 21947-972, Brazil*

² *Institute of Thermal Technology
Silesian University of Technology
Konarskiego 22, 44-100 Gliwice, Poland
e-mail: helcio@mecanica.coppe.ufrj.br*

In this work, we applied the Markov chain Monte Carlo (MCMC) method for the estimation of parameters appearing in the Pennes' formulation of the bioheat transfer equation. The inverse problem of parameter estimation was solved with the simulated transient temperature measurements. A one-dimensional (1D) test case was used to explore the capabilities of using the MCMC method in bioheat transfer problems, specifically for the detection of skin tumors by using surface temperature measurements. The analysis of the sensitivity coefficients was performed in order to examine linear dependence and low sensitivity of the model parameters. The solution of the direct problem was verified with a commercial code. The results obtained in this work show the ability of using inverse heat transfer analysis for the detection of skin tumors.

Keywords: inverse problems, Bayesian framework, Markov chain Monte Carlo method, Pennes' equation, skin tumor.

NOMENCLATURE

c	– specific heat [J/kgK],
h	– heat transfer coefficient [W/m ² K],
k	– thermal conductivity [W/mK],
L	– thickness of the slab [m],
\mathbf{P}	– vector of parameters,
\dot{q}_m	– metabolic heat generation rate [W/m ³],
r	– random number,
t	– time [s],
T	– temperature of the tissue [K],
T_a	– arterial blood temperature [K],
T_∞	– ambient temperature [K],
w	– maximum variation,
\mathbf{W}	– covariance matrix of the measurement errors,
\mathbf{Y}	– vector of measurements.

GREEK SYMBOLS

ε	–	vector of measurements errors,
μ	–	mean value,
$\pi(\mathbf{P})$	–	prior density function,
$\pi(\mathbf{P} \mathbf{Y})$	–	posterior density function,
$\pi(\mathbf{Y})$	–	marginal probability density of the measurements,
$\pi(\mathbf{Y} \mathbf{P})$	–	likelihood function,
ρ	–	density [kg/m ³],
σ	–	standard deviation,
ω	–	perfusion rate [1/s].

SUBSCRIPTS

b	–	blood,
j	–	parameter j ,
max	–	maximum value of the parameter,
min	–	minimum value of the parameter,
t	–	healthy tissue,
tumor	–	tumor tissue,
posterior	–	posterior distribution function.

1. INTRODUCTION

Inverse heat transfer problems, making use of measured temperature, heat flux, radiation intensities, etc., are used for the estimation of unknown quantities appearing in the mathematical formulation of physical processes in thermal sciences. Inverse problems are mathematically classified as ill-posed because their solution might not satisfy the requirements of existence, uniqueness and stability with respect to the input data [25]. An inverse problem is approximately solved through its reformulation to a well-posed problem using some kind of regularization (stabilization) techniques.

Although not always considered in such a way, the solution of inverse problems can be appropriately formulated in terms of statistical inference [31]. Statistical inference refers to the process of drawing conclusions or making predictions based on limited information, beyond the immediately available data [60]. This is exactly what solving inverse problems is intended to do. Many techniques of solving inverse problems are described in the literature, but the most general ones are usually related to the minimization of an objective function depending on the difference between measured and estimated responses to the physical problem [2, 3, 5–7, 9, 11, 28, 31–33, 39, 42, 44–46, 48, 50, 52, 56–59, 60, 62, 67, 69]. If the objective function is derived based on statistical hypotheses for the measurement errors and unknown parameters/functions, the minimization procedure can be related to statistical inference, thus resulting in point estimates for the unknowns that allow for estimations of their associated uncertainties [5, 31]. Unfortunately, this is seldom the case, especially when the objective function is penalized with regularization terms.

In this paper, an inverse parameter estimation problem in bioheat transfer is solved within the Bayesian framework of statistics by using an MCMC method. The term ‘Bayesian’ is commonly used to refer to the techniques for the solution of inverse problems that fall within the framework of statistics developed by the Presbyterian minister, Rev. Thomas Bayes (1702–1761) [35]. Such framework was actually established after Bayes’ death, when his friend, Richard Price, published

Bayes' famous paper, which dealt with the following problem: "*Given the number of times in which an unknown event has happened and failed: Required the chance that the probability of its happening in a single trial lies somewhere between two degrees of probability that can be named*" [4]. On the other hand, the mathematical formulation that is known today as Bayes' theorem is attributed to Laplace [54]. The term 'Bayesian' was first used by R.A. Fisher, but in a pejorative context. Although born more than 120 years after the death of Bayes, Fisher was Bayes' biggest intellectual rival [54]. The Fisher's major issue against Bayes and Laplace was that they used the concept of a prior probability, which represents the information about an unknown quantity before the measured data is available [54]. Fisher's theory relies solely on the measured data and on the modeling of their associated uncertainty, aiming at unbiased inference and/or decision; therefore, it is usually referred to as the frequentist framework in statistics [54, 60, 67]. On the other hand, within the Bayesian framework credit is also given to previous information, in addition to that given to the measured data. Such previous information can even be qualitative, but needs to be represented in terms of a probability distribution function and, regretfully, induces bias in the results [35, 54, 60]. Nevertheless, the use of prior information in the Bayesian framework does not mean that it completely overtakes the information provided by the measured data, unless the latter one is too uncertain to be taken into account. The major source for the solution of inverse problems within the Bayesian framework is the book by Kaipio and Somersalo [31]. In addition, the reader is referred to the book by Gamerman and Lopes [21] for more details about the MCMC methods, and to the books by Lee [35] and Winkler [64] for the fundamentals of Bayesian statistics.

Each human organ has different thermophysical properties, and in almost all organs and tissues (except bones and epidermis) the metabolic heat is produced [17, 29, 49, 53]. The human body, despite the complicated heat transfer processes that occur within it, is kept at a nearly constant core temperature, normally between 36.5°C and 37.1°C , by active thermoregulation [17]. The temperature of the skin depends on the environmental conditions, such as the ambient temperature as well as heat transfer by convection and radiation with the surroundings. The mean temperature of the skin varies from 33.0°C to 34.5°C for men and from 32.2°C to 35.0°C for women. Local skin temperature varies over the body, within the range from 32.0°C to 35.5°C [23, 26]. A classical model for bioheat transfer was proposed by Pennes in 1948 [51]. It involved heat transfer in tissues perfused by blood in small vessels (i.e., without accounting for the heat transfer to/from blood in main arteries and veins). Although various extensions of Pennes' model have been proposed in the literature, its classical model is still used in many cases nowadays. Examples of the of Pennes model extensions were presented, for example, in [10, 16, 18, 20, 63, 66, 68].

Cancerous cells in a solid tumor behave differently from normal cells. The blood perfusion coefficient can be 50 times higher in a tumor than in a healthy tissue, while metabolic heat generation can be respectively 65 times higher [12]. Large tumors which are located in a favorable location can be detected by infrared thermography. Some benefits of using this technique for the detection of tumors in the early stages of growth are described in [33]. In fact, reports can be found where the qualitative analysis of the skin temperature is used for the detection of cancer in the skin [11, 14, 47], breast [8], and thyroid [36, 61, 65]. An extensive review of medical infrared imaging is presented in [15].

Temperature measurements can also be applied together with mathematical modeling in inverse analyses for tumor detection, which is then used for the estimation of the bioheat transfer model parameters [1, 8, 13, 19, 30, 37, 60, 64]. Agnelli et al. [1] used non-invasive thermal diagnostics to estimate unknown thermophysical and geometrical parameters of a tumor. Das et al. [8, 13] estimated the size and location of the tumor described by the classical Pennes equation for 1D, 2D and 3D geometries. However, for the detection of surface tumors the variation of the temperature at the skin surface usually is very small, with changes around 0.55°C or even 0.0077°C [12]. Such small differences make the detection process very difficult because of high probability of false-negative results. Souza et al. [55] solved a function estimation problem, by using the conjugate gradient method with adjoint problem formulation, to identify the blood perfusion coefficient. The authors obtained good results for cases with a low perfusion coefficient. The effective thermal conductivity

and the volumetric heat capacity of a living tissue were simultaneously estimated by Huang and Huang in [30]. Figueiredo and Guimarães [19] used the sequential function specification method for estimating the location and magnitude of a metabolic heat generation term of a 6 cm tissue (1D problem) containing a breast tumor. Umadevi [60] used the Metropolis-Hastings algorithm for estimating the position, size and temperature of a breast tumor and reached very promising results. Inverse methods of state estimation related to the hyperthermia treatment of cancer were addressed in [36, 39, 61].

In this work, we apply an MCMC method [21, 31, 35, 60] within the Bayesian framework, in order to identify parameters appearing in a 1D bioheat transfer problem that involves a single tissue. The objective is the detection of a cancerous tissue, with the initial hypothesis that it is a normal healthy tissue. Bioheat transfer is modeled in terms of Pennes' equation and the simulated temperature measurements are used for the solution of the present inverse parameter estimation problem. The sensitivity coefficients with respect to the different parameters of the model are examined in order to detect small sensitivities and linear dependency in the parameters [38].

2. SOLUTION OF INVERSE PROBLEMS WITHIN THE BAYESIAN FRAMEWORK

Let us consider the vector of parameters appearing in the mathematical formulation of a bioheat transfer problem given by:

$$\mathbf{P}^T = [P_1, P_2, \dots, P_N], \quad (1)$$

where N is the number of parameters. Let us consider also that the transient measurements are available within the medium or at its surface, where the heat transfer processes are being mathematically formulated. The vector containing the measurements is written as

$$\mathbf{Y}^T = (\vec{Y}_1, \vec{Y}_2, \dots, \vec{Y}_I), \quad (2)_1$$

where \vec{Y}_i contains the data of M sensors at time t_i , $i = 1, \dots, I$, that is,

$$\vec{Y}_i = (Y_{i1}, Y_{i2}, \dots, Y_{iM}) \quad \text{for } i = 1, \dots, I, \quad (2)_2$$

so that there are $D = MI$ measurements in total.

We assume that the measurement errors are additive, that is,

$$\mathbf{Y} = \mathbf{T}(\mathbf{P}) + \boldsymbol{\varepsilon}, \quad (3)$$

where $\mathbf{T}(\mathbf{P})$ is the solution of the mathematical formulation of the physical problem, obtained with the vector of parameters \mathbf{P} , that is,

$$\mathbf{T}^T(\mathbf{P}) = [\vec{T}_1(\mathbf{P}), \vec{T}_2(\mathbf{P}), \dots, \vec{T}_I(\mathbf{P})], \quad (4)_1$$

where

$$\vec{T}_i(\mathbf{P}) = [T_{i1}(\mathbf{P}), T_{i2}(\mathbf{P}), \dots, T_{iM}(\mathbf{P})] \quad \text{for } i = 1, \dots, I. \quad (4)_2$$

By further assuming that the measurement errors $\boldsymbol{\varepsilon}$ are Gaussian random variables with zero means, known covariance matrix \mathbf{W} and independent of the parameters \mathbf{P} , their probability density function is given in [5, 9, 21, 31, 32, 44, 46, 56] as

$$\pi(\boldsymbol{\varepsilon}) = \pi(\mathbf{Y} | \mathbf{P}) = (2\pi)^{-D/2} |\mathbf{W}|^{-1/2} \exp \left\{ -\frac{1}{2} [\mathbf{Y} - \mathbf{T}(\mathbf{P})]^T \mathbf{W}^{-1} [\mathbf{Y} - \mathbf{T}(\mathbf{P})] \right\}, \quad (5)$$

which is the *likelihood function* for the studied case. The likelihood function gives the relative probability density of different measurement outcomes \mathbf{Y} with a fixed \mathbf{P} [5, 9, 21, 31, 32, 44, 46, 56].

For the solution of inverse problems within the Bayesian framework, all variables included in the mathematical formulation of the physical problem are modeled as random variables. Techniques for the solution of inverse problems within the Bayesian framework can be summarized in the following steps [31]:

1. Based on all information available for the parameters \mathbf{P} before the measured data \mathbf{Y} is taken, select a probability distribution function $\pi(\mathbf{P})$ that appropriately represents the prior information.
2. Select the likelihood function $\pi(\mathbf{Y} | \mathbf{P})$ that appropriately models the measurement errors and involves a relationship between the observations and the mathematical model of the physical problem under study, cf. Eq. (5).
3. Develop methods to explore the posterior density function which is the conditional probability distribution of the unknown parameters given the measurements $\pi(\mathbf{P} | \mathbf{Y})$.

The formal mechanism to combine the new information (measurements) with the previously available information (prior) is known as Bayes' theorem [5, 9, 21, 31, 32, 44, 46, 56]. Let \mathbf{P} and \mathbf{Y} be continuous random variables. Then, we can write [60]:

$$\pi(\mathbf{P} | \mathbf{Y}) = \frac{\pi(\mathbf{P}, \mathbf{Y})}{\pi(\mathbf{Y})}, \quad (6)$$

that is, the conditional density of the random variable \mathbf{P} given a value of the random variable \mathbf{Y} is the joint density of \mathbf{P} and \mathbf{Y} divided by the marginal density of \mathbf{Y} , where

$$\pi(\mathbf{Y}) = \int_{R^N} \pi(\mathbf{P}, \mathbf{Y}) d\mathbf{P}. \quad (7)$$

The joint density $\pi(\mathbf{P}, \mathbf{Y})$ is not generally known, but it can be written in terms of the likelihood and the prior as [60]:

$$\pi(\mathbf{P}, \mathbf{Y}) = \pi(\mathbf{Y} | \mathbf{P})\pi(\mathbf{P}). \quad (8)$$

By substituting Eq. (8) into Eq. (6) we obtain Bayes' theorem, which is given by

$$\pi_{\text{posterior}}(\mathbf{P}) = \pi(\mathbf{P} | \mathbf{Y}) = \frac{\pi(\mathbf{Y} | \mathbf{P})\pi(\mathbf{P})}{\pi(\mathbf{Y})}. \quad (9)$$

Since the computation of $\pi(\mathbf{Y})$ with Eq. (7) is in general difficult, and usually not needed for practical calculations as will be apparent below, Bayes' theorem is commonly written as

$$\pi_{\text{posterior}}(\mathbf{P}) = \pi(\mathbf{P} | \mathbf{Y}) \propto \pi(\mathbf{Y} | \mathbf{P})\pi(\mathbf{P}). \quad (10)$$

Analytical posterior distributions might be obtained when the prior is conjugate to the likelihood [21, 31, 35, 60], which would allow for the solution of the inverse problem in terms of a point estimate for \mathbf{P} through an optimization problem that maximizes the posterior distribution, that is,

$$\mathbf{P}_{\text{MAP}} = \arg \max_{\mathbf{P} \in R^N} \pi(\mathbf{P} | \mathbf{Y}), \quad (11)$$

which is usually referred to as a *maximum a posteriori* estimation.

On the other hand, other point and confidence estimates from the posterior distribution typically require numerical integration. For example, one common point estimate is the *conditional mean* defined as [31]:

$$\mathbf{P}_{\text{CM}} = E(\mathbf{P}) = \int_{R^N} \mathbf{P} \pi(\mathbf{P} | \mathbf{Y}) d\mathbf{P}, \quad (12)$$

where $E(\cdot)$ denotes the expected value. In general, the dimension N of the parameter space is large enough to make the numerical integration in Eq. (12) impractical. Besides that, the computation of the normalizing constant in the denominator of $\pi(\mathbf{P} | \mathbf{Y})$ (see Eq. (9)) already constitutes a challenging problem by itself. For the cases in which the posterior is not analytical and/or numerical integrations required for estimates are not practical, the MCMC methods can provide a solution of the inverse problem, so that inference on the posterior probability becomes inference on its samples [1, 9, 21, 31, 32, 44, 46, 56, 60]. For example, the Monte Carlo integration of Eq. (12) can be approximated by [31]:

$$\mathbf{P}_{\text{CM}} = E(\mathbf{P}) = \int_{R^N} \mathbf{P} \pi(\mathbf{P} | \mathbf{Y}) d\mathbf{P} \approx \frac{1}{n} \sum_{t=1}^n \mathbf{P}^{(t)}, \quad (13)$$

where $\mathbf{P}^{(t)}$, for $t = 1, \dots, n$, are the samples from $\pi(\mathbf{P} | \mathbf{Y})$. The MCMC methods are used to obtain such samples.

Due to the simplicity of the application of MCMC methods, such a technique for the solution of inverse problems has recently become quite popular, being applied even for the cases in which a maximum a posteriori probability (MAP) estimate is feasible. One clear disadvantage of the application of Monte Carlo methods is the required long computational time. On the other hand, the use of computationally fast reduced models of the physical problem can be appropriately accommodated within the Bayesian framework [31], so that the application of MCMC methods for many practical problems is nowadays possible.

The most common MCMC algorithms are the Gibbs sampler and the Metropolis-Hastings algorithm [9, 21, 31, 32, 35, 41, 46, 56, 60]. The Metropolis-Hastings algorithm, which was used in this work, was first proposed by Metropolis et al. [41] in 1953, who aimed at the calculation of the properties of substances composed of interacting molecules. It was, therefore, a work focused on statistical mechanics, and not on statistics itself. Although the paper has five co-authors [41], only the name of the first author became popular to designate the developed algorithm, which was later generalized by Hastings in 1970 [27].

The implementation of the Metropolis-Hastings algorithm starts with the selection of a candidate or proposal distribution $q(\mathbf{P}^* | \mathbf{P}^{(t)})$, which is used to draw a new candidate state \mathbf{P}^* , given the current state $\mathbf{P}^{(t)}$ is of the Markov chain. The balance (reversibility) condition of the Markov chain of interest is given by:

$$\pi_{\text{posterior}}(\mathbf{P}^{(t)}) q(\mathbf{P}^* | \mathbf{P}^{(t)}) = \pi_{\text{posterior}}(\mathbf{P}^*) q(\mathbf{P}^{(t)} | \mathbf{P}^*). \quad (14)$$

In order to avoid possible cases in which $\pi_{\text{posterior}}(\mathbf{P}^{(t)}) q(\mathbf{P}^* | \mathbf{P}^{(t)}) > \pi_{\text{posterior}}(\mathbf{P}^*) q(\mathbf{P}^{(t)} | \mathbf{P}^*)$, that is, the process moves from $\mathbf{P}^{(t)}$ to \mathbf{P}^* more often than the reverse, a probability $\alpha(\mathbf{P}^* | \mathbf{P}^{(t)})$ is introduced in Eq. (14), so that [35]:

$$\pi_{\text{posterior}}(\mathbf{P}^{(t)}) q(\mathbf{P}^* | \mathbf{P}^{(t)}) \alpha(\mathbf{P}^* | \mathbf{P}^{(t)}) = \pi_{\text{posterior}}(\mathbf{P}^*) q(\mathbf{P}^{(t)} | \mathbf{P}^*). \quad (15)$$

Therefore,

$$\alpha(\mathbf{P}^* | \mathbf{P}^{(t)}) = \min \left[1, \frac{\pi_{\text{posterior}}(\mathbf{P}^*) q(\mathbf{P}^{(t)} | \mathbf{P}^*)}{\pi_{\text{posterior}}(\mathbf{P}^{(t)}) q(\mathbf{P}^* | \mathbf{P}^{(t)})} \right], \quad (16)$$

where $\alpha(\mathbf{P}^* | \mathbf{P}^{(t)}) = 1$ holds/remains valid when the balance (reversibility) condition is satisfied. Equation (16) is also called the Metropolis-Hastings ratio. For the computation of Eq. (16), we notice that there is no need to know the normalizing constant that appears in the definition of the posterior distribution (see Eq. (9)).

In the Metropolis-Hastings algorithm, a candidate \mathbf{P}^* is accepted based on the probability $\alpha(\mathbf{P}^* | \mathbf{P}^{(t)})$. The Metropolis-Hastings algorithm is summarized in the following steps [9, 21, 31, 32, 35, 41, 44, 46, 56, 60]:

1. Let $t = 1$ and start the Markov chain with the initial state $\mathbf{P}^{(1)}$.
2. Sample a candidate point \mathbf{P}^* from a proposal distribution $q(\mathbf{P}^* | \mathbf{P}^{(t)})$.
3. Calculate the probability $\alpha(\mathbf{P}^* | \mathbf{P}^{(t)})$ with Eq. (16).
4. Generate a random value $U \sim U(0,1)$, which is uniformly distributed in $(0,1)$.
5. If $U \leq \alpha(\mathbf{P}^* | \mathbf{P}^{(t)})$, set $\mathbf{P}^{(t+1)} = \mathbf{P}^*$. Otherwise, set $\mathbf{P}^{(t+1)} = \mathbf{P}^{(t)}$.
6. Make $t = t + 1$ and return to step 2 in order to generate the sequence $\{\mathbf{P}^{(1)}, \mathbf{P}^{(2)}, \dots, \mathbf{P}^{(n)}\}$.

In this way, a sequence is generated to represent the posterior distribution and inference on this distribution is obtained from inference on the samples $\{\mathbf{P}^{(1)}, \mathbf{P}^{(2)}, \dots, \mathbf{P}^{(n)}\}$. We note that the values of $\mathbf{P}^{(t)}$ must be ignored until the chain has not converged to equilibrium (the burn-in period).

The proposal distribution plays a fundamental role for the success of the Metropolis-Hastings algorithm. Typical choices for $q(\mathbf{P}^* | \mathbf{P}^{(t)})$ are random walk processes or independent moves based on the priors, but adaptive proposal distributions can also be used, as proposed by Haario [24].

3. PHYSICAL PROBLEM AND MATHEMATICAL FORMULATION

The physical problem examined here is related to the studies in [11], in which skin cancer is detected through the qualitative analysis of the transient superficial skin temperature, after a thermal perturbation is imposed. Typically, the thermal perturbation is caused by a cooling of the skin surface, which can be performed by different means, and then measuring the skin surface temperature with an infrared camera [47]. The mathematical model of local skin cooling was validated in [47], being part of a larger project of temperature measurements during reheating, with a target to distinguish malignant from non-malignant tumors [47]. Reheating occurs naturally, due to the heat conduction in the tissue, metabolic heat generation, blood perfusion and heat transfer of the skin with the surrounding environment.

A 1D case is analyzed in this work, representing heat transfer in a skin layer. The medium is considered as a slab of thickness L , with the internal surface maintained at the constant temperature T_a (the arterial blood temperature). The other surface is exposed to the surrounding, at the ambient temperature T_∞ . Heat is transferred between the skin surface and the surrounding by convection and linearized radiation, with the heat transfer coefficient h . Such steady-state solution is used as initial state of cooling process. The skin layer is perturbed from its steady-state temperature through the perfect contact of its surface with a thermal reservoir at 0°C , during 15 seconds ($-15 \text{ s} < t < 0 \text{ s}$). The temperature distribution in the skin layer after this cooling period, represented by $F(x)$, serves as the initial condition for the reheating period, which is the subject of the current analysis. Measurements of the temperature evolution of the skin surface are assumed to be available during 50 seconds in the reheating period.

For the present 1D problem, Pennes' model for bioheat transfer is given by:

$$\rho c \frac{\partial T}{\partial t} = \frac{\partial}{\partial x} \left(k \frac{\partial T}{\partial x} \right) + \omega_b \rho_b c_b (T_a - T) + \dot{q}_m \quad \text{in } 0 < x < L \quad \text{for } t > 0. \quad (17)_1$$

The boundary and initial conditions are given by:

$$T = T_a \quad \text{at } x = 0 \quad \text{for } t > 0, \quad (17)_2$$

$$k \frac{\partial T}{\partial x} + hT = hT_\infty \quad \text{at } x = L \quad \text{for } t > 0, \quad (17)_3$$

$$T = F(x) \quad \text{in } 0 < x < L \quad \text{for } t = 0. \quad (17)_4$$

In the direct problem, all parameters appearing in Eq. (17) are considered as known; the objective of the direct problem is to determine the transient temperature variation in the skin layer. The inverse problem examined here is focused on the estimation of the thermal parameters appearing in Eq. (17)₁ by using the transient temperature measurements taken at the surface $x = L$. The inverse problem solution is recast as statistical inference in the Bayesian framework of statistics, by using the Metropolis-Hastings algorithm described earlier in this paper and by assuming that the temperature measurement errors follow the Gaussian distribution given by Eq. (5).

4. RESULTS AND DISCUSSION

For the results presented below, the thermal parameters for the tissue layer were considered to be constant. The values used for the model parameters, in order to perform the sensitivity analysis and generate the simulated measurements, are presented in Table 1 [11, 17, 47]. For the tumor, the blood perfusion coefficient was assumed as five times larger and the metabolic heat generation rate as ten times larger than those of the healthy tissue [11]. The initial condition for the problem was assumed as the solution of problem (17) after the skin surface at $x = L$ was maintained at 0°C for 15 seconds.

Table 1. Model parameters [11, 17, 44].

Parameter	Value
L	0.005 m
T_a	37°C
h	10 Wm ⁻² K ⁻¹
T_∞	23°C
$\rho_t = \rho_{\text{tumor}}$	1085 kgm ⁻³
$c_t = c_{\text{tumor}}$	3680 Jkg ⁻¹ K ⁻¹
$k_t = k_{\text{tumor}}$	0.47 Wm ⁻¹ K ⁻¹
c_b	3617 Jkg ⁻¹ K ⁻¹
ρ_b	1060 kgm ⁻³
$\omega_{b,t}$	0.00105 s ⁻¹
$\omega_{b, \text{tumor}}$	0.00525 s ⁻¹
$\dot{q}_{m,t}$	631.0 Wm ⁻³
$\dot{q}_{m, \text{tumor}}$	6310.0 Wm ⁻³

In this work, the solution of the direct problem was computed by using the central difference, fully implicit finite volume method, which was implemented in the MATLAB platform [40]. A grid independency analysis was made and 27 volumes were chosen for the spatial discretization, while a time step of 0.05 s was used, for a final time of 50 s. The results obtained for the direct problem with the code developed in this work were verified with the numerical solution of the ANSYS package.

Before the estimation of the model parameters is attempted, the analysis of the sensitivity coefficients needs to be performed in order to detect the linearly dependent parameters as well as the parameters with small sensitivities with respect to the measurements [5]. The analysis of the sensitivity coefficients is more appropriately performed with the reduced sensitivity coefficients that are defined as [5]:

$$J_{P_j} = P_j \frac{\partial T}{\partial P_j}, \quad (18)$$

where P_j , $j = 1, \dots, N$, are the unknown parameters. In Eq. (18), we note that the unit of the reduced sensitivity coefficients is the same as unit of T ; hence, the magnitude of the sensitivity coefficients can be compared to the magnitudes of the temperature measurements, which are considered to be non-invasively taken at the skin surface ($x = L$). Before performing the analysis of the sensitivity coefficients, we note in Eqs. (17)₁–(17)₄ that not all the parameters appear independently in the mathematical formulation, for example, the parameters in the groups (ρc) and $(\omega_b \rho_b c_b)$. Therefore, the model parameters for this problem are written as

$$\mathbf{P}^T = [A, B, C, D, h, T_\infty, T_a], \quad (19)$$

where

$$A = (\rho c), \quad B = k, \quad C = (\omega_b \rho_b c_b) \quad \text{and} \quad D = \dot{q}_m.$$

The analysis of the sensitivity coefficients is focused on the parameters of main interest for the problem, which are the skin thermophysical properties represented by A , B , C and D . Figures 1a and 1b show the sensitivity coefficients with respect to these parameters, as a function of time, for the case involving healthy and tumorous tissues, respectively. The surface temperatures are also presented in Fig. 1. As it can be noticed, the sensitivity coefficients with respect to the parameters A , B and D are practically null and much smaller than those for the parameter C , in both cases of healthy and tumorous tissues. Therefore, the estimation of the parameter C , which is related to the blood perfusion in the tissue, should be the focus for the detection of a skin cancer in the problem examined in this work.

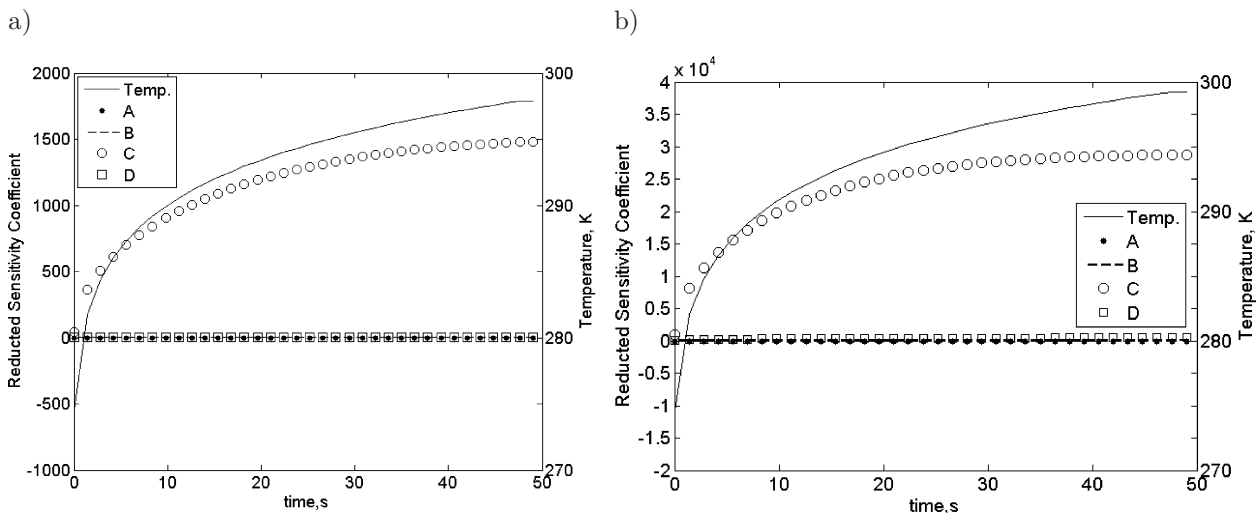


Fig. 1. Sensitivity coefficients at $x = L$ for: a) healthy skin tissue, b) tumorous skin tissue.

From the analysis of the sensitivity coefficients, which revealed that the surface temperature is practically not affected by A , B and D , prior densities in the form of truncated Gaussian distribu-

tions were assumed for these parameters. For a single parameter P_j , the truncated Gaussian prior with mean μ_j and variance σ_j^2 is given by:

$$\pi(P_j) \propto \left[-\frac{1}{2} \frac{(P_j - \mu_j)^2}{\sigma_j^2} \right] \quad \text{for } P_{j,\min} \leq P_j \leq P_{j,\max}, \quad (20)$$

$$\pi(P_j) = 0 \quad \text{for } P_j < P_{j,\min} \quad \text{or} \quad P_j > P_{j,\max}.$$

For each parameter A , B and D , μ_j was taken as the exact value used to generate the simulated measurements obtained from Table 1, $\sigma_j = 0.0005\mu_j$, $P_{j,\min} = 0.9\mu_j$, and $P_{j,\max} = 1.1\mu_j$. In order to challenge the estimation procedure used in this work, the prior distribution for the parameter C was taken as a uniform distribution in $0 < C < 40257.21 \text{ Wm}^{-3}\text{K}^{-1}$, where the upper bound corresponds to twice the exact value for the tumorous tissue. Therefore, the uniform prior encompasses the exact values for the healthy tissue ($C = 4025.72 \text{ Wm}^{-3}\text{K}^{-1}$) and the tumor tissue ($C = 20128.61 \text{ Wm}^{-3}\text{K}^{-1}$). The parameters h , T_∞ , T_a were assumed as deterministically known for the results presented below.

Simulated temperature measurements were used in this paper, obtained from a Gaussian uncorrelated distribution, with a zero mean and a constant standard deviation $\sigma = 0.3 \text{ K}$. The simulated measurements are presented in Fig. 2, together with the exact temperatures obtained from the solution of problem (17) with the parameters specified in Table 1, for the cases of healthy tissue and tumorous tissue, respectively. We notice that, at the 99% confidence level, the measurement errors may reach 3% of the maximum temperature difference observed during the reheating process.

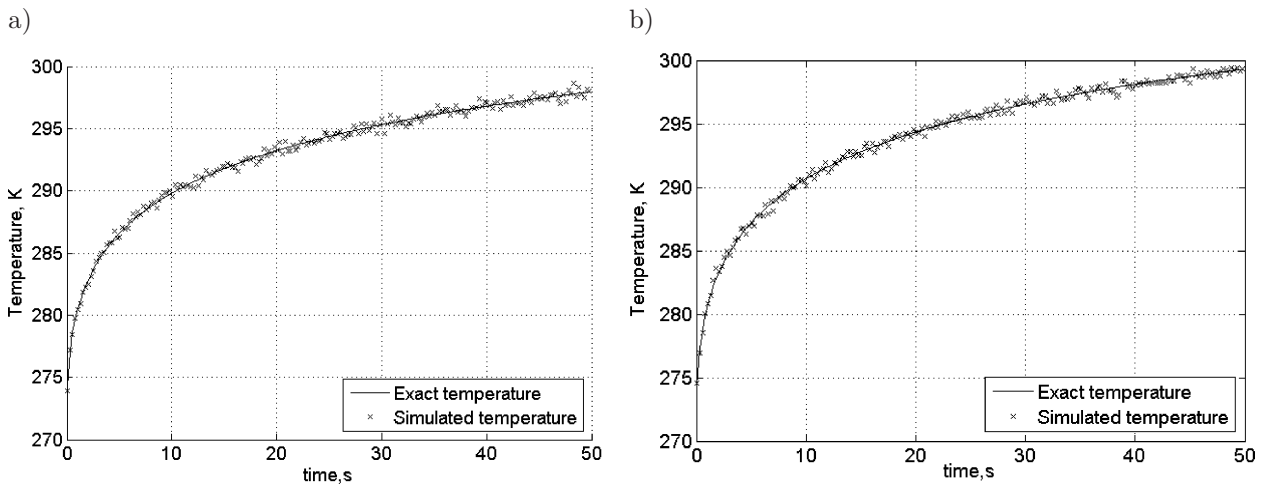


Fig. 2. Exact temperatures and simulated measurements: a) in the healthy skin tissue, b) in the tumorous skin tissue.

For the implementation of the Markov chains, a random walk proposal was used in this work in the following form:

$$P_j^* = P_j^{(t)} + w_j(2r_j - 1) \quad \text{for } j = 1, \dots, N = 4, \quad (21)$$

where r_j is a random number with uniform distribution in $(0, 1)$, that is, $r_j \sim U(0, 1)$, while w_j is the maximum variation for the parameter P_j that is given in Table 2.

The convergence of the Markov chain to an equilibrium distribution can be verified by plotting the chains of each parameter $\{P_j^{(1)}, P_j^{(2)}, \dots, P_j^{(n)}\}$, $j = 1, \dots, N$, and the posterior distribution

Table 2. Maximum variation for the proposal distributions of each parameter.

Parameter	A [$\text{Jm}^{-3}\text{K}^{-1}$]	B [$\text{Wm}^{-1}\text{K}^{-1}$]	C [$\text{Wm}^{-3}\text{K}^{-1}$]	D [Wm^{-3}]
For healthy skin tissue	79.86	9.4×10^{-6}	0.28	0.081
For tumorous skin tissue	79.86	9.4×10^{-6}	1.41	0.403

$\pi_{\text{posterior}}(\mathbf{P}^{(t)})$, $t = 1, \dots, n$. The convergence of the Markov chain can also be verified by the method proposed by Geweke [22]. Let

$$\bar{P}_j^a = \frac{1}{s_a} \sum_{r=1}^{s_a} P_j^{(r)} \tag{22}$$

and

$$\bar{P}_j^b = \frac{1}{s_b} \sum_{r=s^*}^n P_j^{(r)} \tag{23}$$

be the means of the samples taken at the beginning and at the end of the supposedly converged chain. Geweke [22] recommended:

$$s^* = n - s_b + 1, \quad s_a = 0.1n, \quad s_b = 0.5n, \tag{17}$$

so that $(\bar{P}_j^a - \bar{P}_j^b) \rightarrow 0$ when the chain $\{P_j^{(1)}, P_j^{(2)}, \dots, P_j^{(n)}\}$ approaches equilibrium.

The results presented below for each parameter are relative to their exact values; hence, an accurate estimation of the parameters is represented by mean values close to unity. We start with the estimation of parameters for the healthy tissue. The Markov chains were started at the mean values of the priors for the parameters, and 200 000 states were simulated in the Markov chains, with a burn-in period of 60 000 states. The converged Markov chains for parameters A , B , C and D are shown in Figs. 3a, 4a, 5a and 6a, respectively, while Figs. 3b, 4b, 5b and 6b present the histograms of the converged states for these parameters. We notice in these figures that the marginal posterior distributions resemble Gaussian distributions. Figure 5 show that the posterior distribution for parameter C for the healthy tissue is not centered around the expected value of unity, but around 1.381. In fact, although the chain was started at the exact value, it converged to a value 38% larger, probably due to the large measurement errors used for the simulations. In any

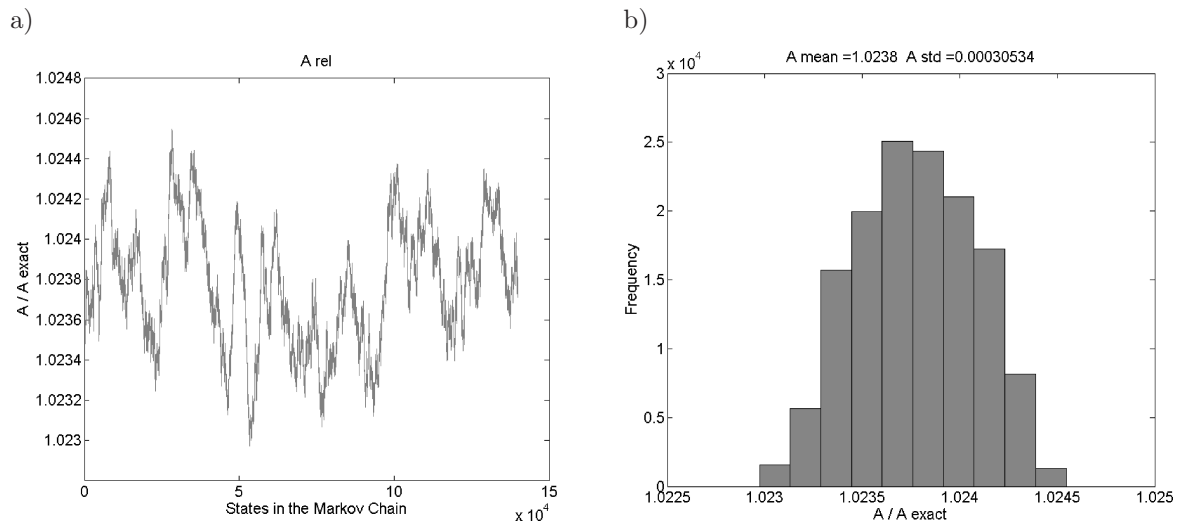


Fig. 3. a) Converged Markov chain for parameter A for the healthy tissue, b) marginal posterior for parameter A for the healthy tissue.

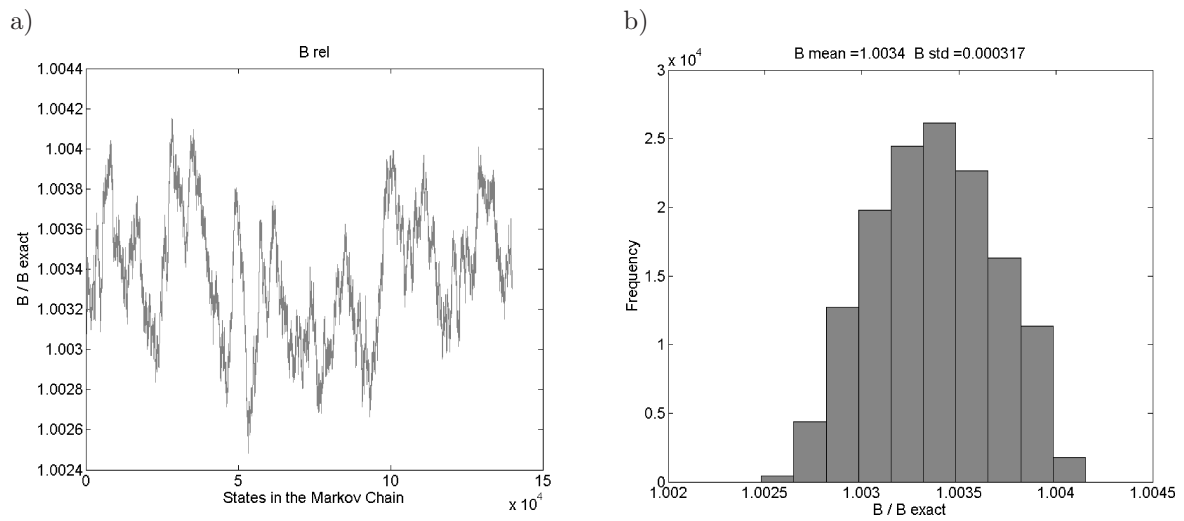


Fig. 4. a) Converged Markov chain for parameter B for the healthy tissue, b) marginal posterior for parameter B for the healthy tissue.

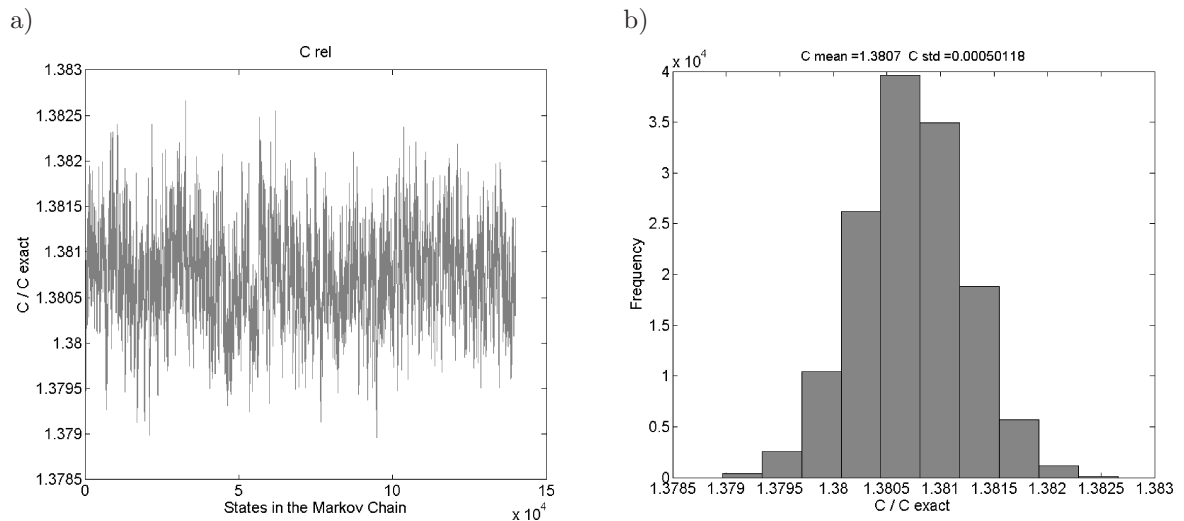


Fig. 5. a) Converged Markov chain for parameter C for the healthy tissue, b) marginal posterior for parameter C for the healthy tissue.

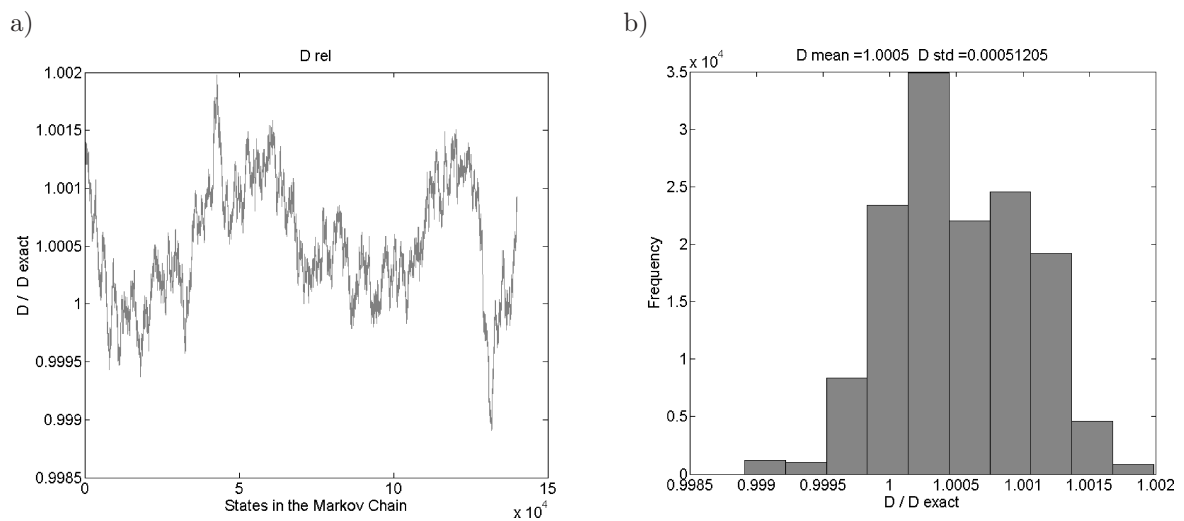


Fig. 6. a) Converged Markov chain for parameter D for the healthy tissue, b) marginal posterior for parameter D for the healthy tissue.

case, the value estimated for C is still much smaller than that related to a tumorous tissue, which is at least five times larger than that of the healthy tissue. Hence, the estimated parameter C would still not suggest the existence of a tumor instead of the healthy tissue. The whole Markov chain for parameter C , including the burn-in period, is presented in Fig. 7.

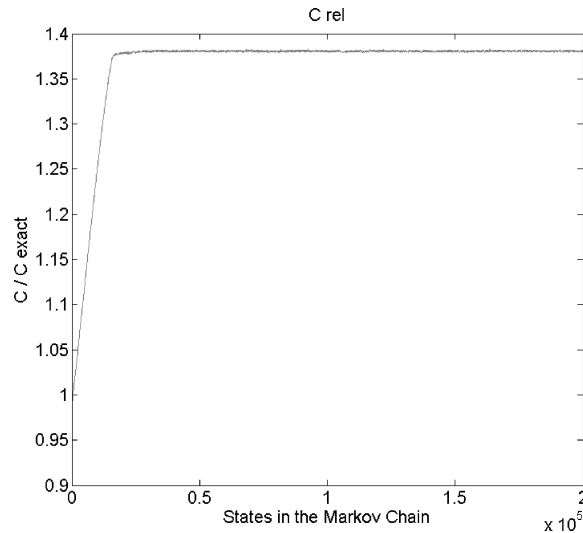


Fig. 7. Markov chain for parameter C for the healthy tissue with the burn-in period.

In order to verify Geweke's criterion for the convergence of the Markov chains, the means of the states were computed at the beginning and at the end of the chains, as given by Eqs. (22) and (23). The results obtained for the four parameters are presented in Fig. 8, where the parameter indexes refer to $P_1 = A$, $P_2 = B$, $P_3 = C$, and $P_4 = D$. This figure shows that, at the graph scale, the means at the beginning and at the end of the chains are perfectly coincident.

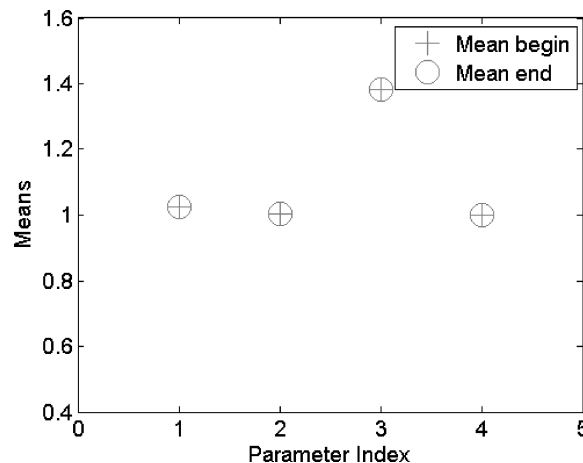


Fig. 8. Means of the states at the beginning and at the end of the Markov chains for the healthy tissue to verify Geweke's criterion.

After estimating the healthy tissue parameters, we examine the possibility of estimating the parameters of the tumorous tissue by starting the Markov chains with the values of the healthy tissue, that is, the tissue is initially assumed as healthy and it is expected that the information provided by the measurements is capable of actually identifying a tumorous tissue. As for the case involving the healthy tissue presented above, 200 000 states were simulated in the Markov chains

and 60 000 states were discarded in the burn-in period. The estimations are presented relative to their exact parameter values.

The Markov chain for parameter C for the tumorous tissue is shown in Fig. 9. In this figure, let us note that the chain, which starts from the value for the healthy tissue, gradually approaches the value of the tumorous tissue that is about five times larger. The converged Markov chains for parameters A , B , C , and D are presented in Figs. 10a, 11a, 12a and 13a. The histograms of the converged marginal posteriors can be found in Figs. 10b, 11b, 12b and 13b. As for the case with the healthy tissue, the histograms of the parameters estimated for the tumorous tissue resemble Gaussian distributions. The convergence of the Markov chains for the tumorous tissue can be verified through the analysis of Geweke's criterion, as shown in Fig. 14.

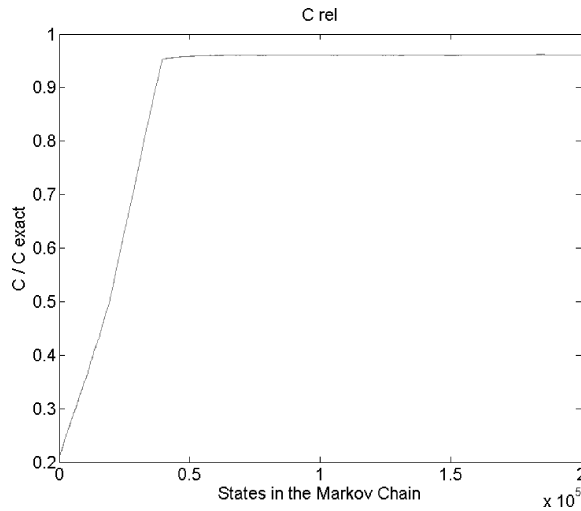


Fig. 9. Markov chain for parameter C for the tumorous tissue.

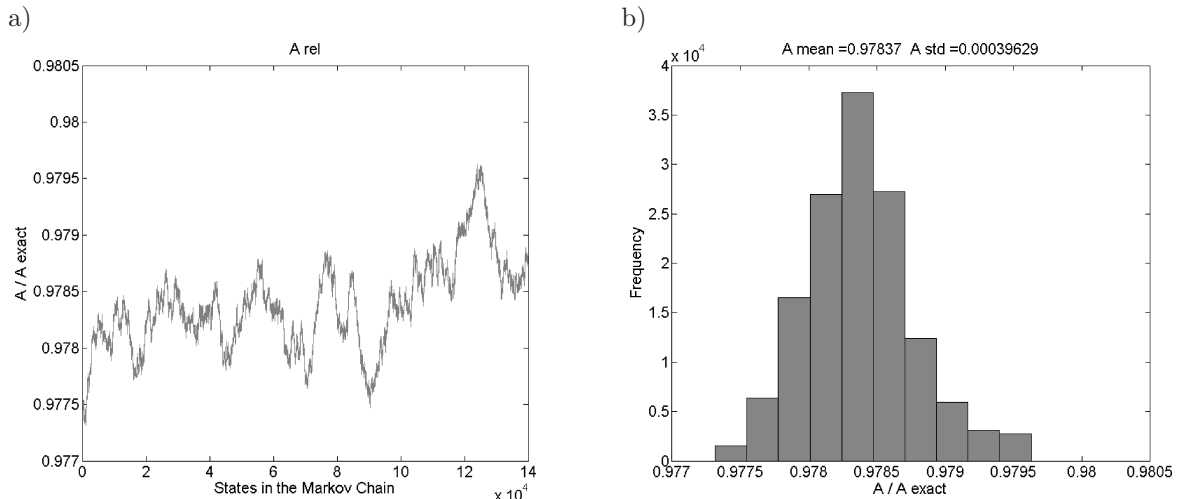


Fig. 10. a) Converged Markov chain for parameter A for the tumorous tissue, b) marginal posterior for parameter A for the tumorous tissue.

The means and the standard deviations of the states of the converged Markov chains for the estimated parameters for the tumorous tissue are shown in Table 3. This table and Figs. 10 to 13 show that all the states in the Markov chains exhibit small standard deviations, although the estimated means are less than 4% off the exact values. In fact, despite the fact that the value of the parameter C was not exactly recovered, the estimated mean for this parameter clearly indicates the tissue with a tumor.

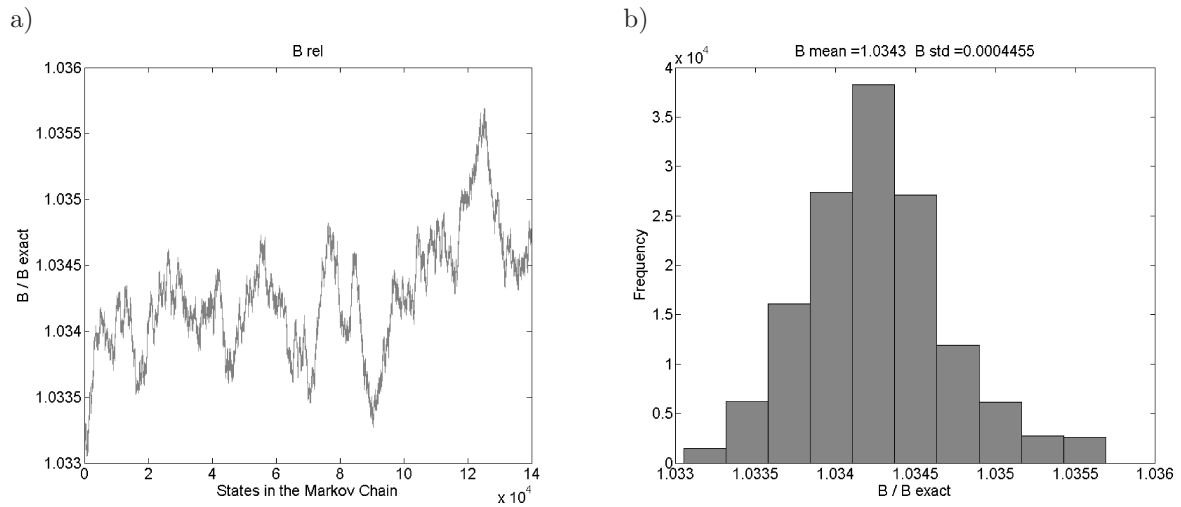


Fig. 11. a) Converged Markov chain for parameter B for the tumorous tissue, b) marginal posterior for parameter B for the tumorous tissue.

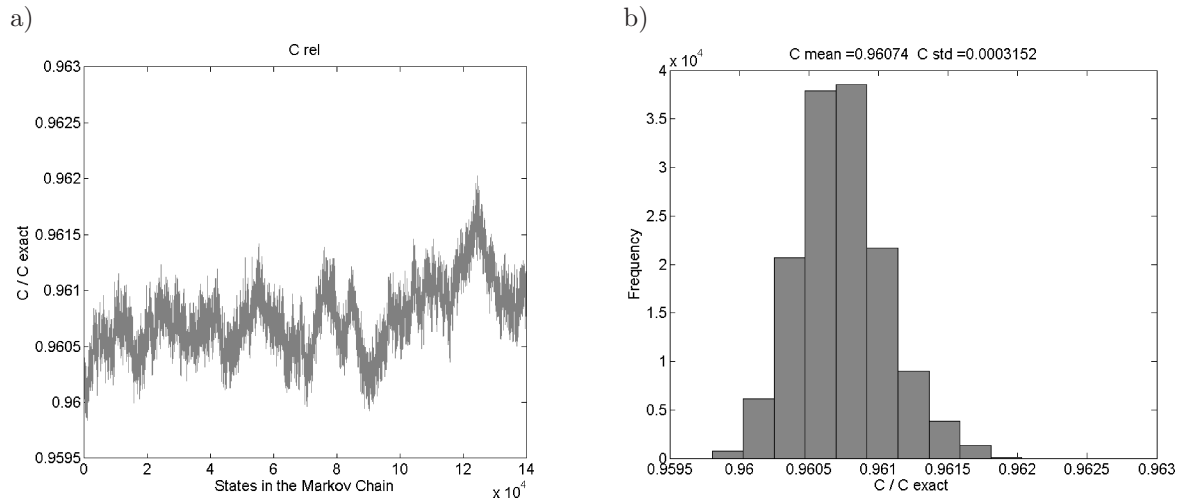


Fig. 12. a) Converged Markov chain for parameter C for the tumorous tissue, b) marginal posterior for parameter C for the tumorous tissue.

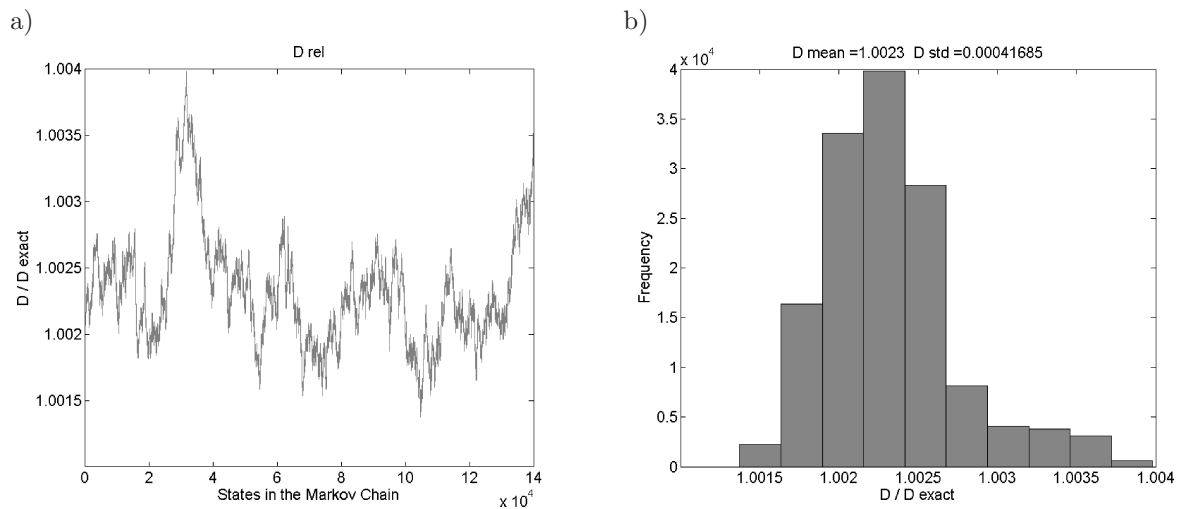


Fig. 13. a) Converged Markov chain for parameter D for the tumorous tissue, b) marginal posterior for parameter D for the tumorous tissue.

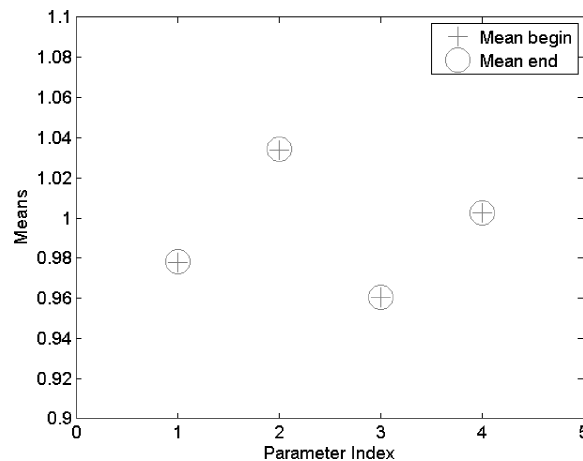


Fig. 14. Means of the states at the beginning and at the end of the Markov chains for the tumorous tissue to verify Geweke's criterion.

Table 3. Means and standard deviations (SD) of the states of the converged Markov chains for the tumorous tissue.

Parameter	A (SD)	B (SD)	C (SD)	D (SD)
Relatives values	0.9784 (4×10^{-4})	1.0343 (4×10^{-4})	0.9607 (3×10^{-4})	1.0023 (4×10^{-4})
Dimensional values	3906 436 (1582) $\text{Jm}^{-3}\text{K}^{-1}$	0.4861 (0.0002) $\text{Wm}^{-1}\text{K}^{-1}$	19 338 (6) $\text{Wm}^{-3}\text{K}^{-1}$	6 325 (3) Wm^{-3}

The results for the healthy and tumorous tissues presented above show that the parameters A , B and D were accurately estimated, despite the fact that their sensitivity coefficients are quite small. This can be explained by using informative priors for the estimation procedure. Nevertheless, the analysis of the sensitivity coefficients shows that the surface temperature is not significantly affected by such parameters, for the values examined in this work, which fairly represent skin properties reported in the literature [11, 17, 44].

Although the estimated mean for the parameter C of the healthy tissue was 38% larger than its exact value, in the case involving the tumorous tissue the mean was only 4% smaller than its exact value. For both cases, the Markov chains were started with the value for the healthy tissue. Therefore, the results presented above reveal that, although the exact value for the healthy tissue could not be recovered, the parameter C estimated in this case was much smaller than the one associated with a tumorous tissue, thus correctly suggesting that the tissue was not tumorous (that is, a false positive detection of cancer is not likely). In the case involving the tumorous tissue, the Markov chain for the parameter C correctly evolved from the initial value associated with the healthy tissue to the value of the tumorous tissue, which was five times larger. Hence, the tumorous tissue could be appropriately detected with the present approach for the solution of inverse parameter estimation problems in bioheat transfer.

5. CONCLUSIONS

This paper dealt with the solution of an inverse parameter estimation problem in bioheat transfer, which aims at the detection of cancer in a single, tumorous or non-tumorous, skin layer. This simplification has caused preliminary investigation and the MCMC testing for those applications. The physical problem under the analysis involved the cooling of the surface of the skin and monitoring its temperature during the reheating caused by perfusion, metabolism and surface convective/radiative heat transfer. The parameters were estimated within the Bayesian framework by

using the Metropolis-Hastings implementation of the MCMC method. The results obtained with the simulated transient measurements of the surface temperature show that the estimates of a parameter associated with the perfusion rate could characterize a cancerous tissue, even when starting the Markov chains at the values of a healthy tissue. More realistic cases involving a multidimensional problem and the actual surface temperature measurements with an infrared camera are currently being undertaken. However, the results obtained with the simple cases examined in this work are encouraging, because the false positive detection of cancer could be avoided and, more importantly, a tumorous tissue could be appropriately detected.

ACKNOWLEDGEMENTS

The authors would like to acknowledge the financial support provided by CNPq, CAPES, FAPERJ, the Ministry of Science and Higher Education of Poland (within statutory research funding scheme) and the Brazilian agency for the fostering of sciences. In addition, we would like to extend our thanks to COPPE/UFRJ and to the Institute of Thermal Technology/SUT. The access provided to the computational facilities of the Division of Physics/SUT is greatly appreciated.

REFERENCES

- [1] J.P. Agnelli, A.A. Barrea, C.V. Turner. Tumor location and parameter estimation by thermography. *Mathematical and Computer Modelling*, **53**: 1527–1534, 2011.
- [2] O.M. Alifanov. *Inverse Heat Transfer Problems*, Springer-Verlag, New York, 1994.
- [3] O.M. Alifanov, E. Artyukhin, A. Rumyantsev. *Extreme Methods for Solving Ill-Posed Problems with Applications to Inverse Heat Transfer Problems*. Begell House, New York, 1995.
- [4] T. Bayes. An Essay towards solving a problem in the doctrine of chances, by the late Rv. Mr. Bayes, F.R.S. Communicated by Mr. Price in a letter to John Cannon. *A.M.R.F.S., Phil. Trans.*, **53**: 370–418, 1763.
- [5] J. Beck, K.J. Arnold. *Parameter Estimation in Engineering and Science*. Wiley Interscience, New York, 1977.
- [6] J.V. Beck, B. Blackwell, C.R. St. Clair. *Inverse Heat Conduction: Ill-Posed Problems*. Wiley Interscience, New York, 1985.
- [7] M. Bertero, P. Boccacci. *Introduction to Inverse Problems in Imaging*. Institute of Physics Publishing, 1998.
- [8] L.A. Bezerra, M.M. Oliveira, T.L. Rolim, A. Conci, F.G.S. Santos, P.R.M. Lyra, R.C.F. Lima. Estimation of breast tumor thermal properties using infrared images. *Signal Processing*, **93**: 2851–2863, 2013.
- [9] D. Calvetii, E. Somersalo. *Introduction to Bayesian Scientific Computing*, Springer, New York, 2007.
- [10] C.K. Charny. Mathematical models of bioheat transfer. [In:] *Advances in Heat Transfer*, Young Cho [Ed.], **22**: 19–156, Boston: Academic Press, 1992.
- [11] Tze-Yuan Cheng, C. Herman. Analysis of skin cooling for quantitative dynamic infrared imaging of near-surface lesions. *International Journal of Thermal Sciences*, **86**: 175–188, 2014.
- [12] K. Das, S.C. Mishra. Estimation of tumor characteristics in a breast tissue with known skin surface temperature. *Journal of Thermal Biology*, **38**: 311–317, 2013.
- [13] K. Das, S.C. Mishra. Non-invasive estimation of size and location of a tumor in a human breast using a curve fitting technique. *International Communications in Heat and Mass Transfer*, **56**: 63–70, 2014.
- [14] K. Das, R. Singh, S.C. Mishra. Numerical analysis for determination of the presence of a tumor and estimation of its size and location in a tissue. *J. Therm. Biol.*, **38**: 32–40, 2013.
- [15] M. Diakides, J.D. Bronzino, D.R. Peterson. *Medical Infrared Imaging: Principles and Practices*, CRC Press, 2013.
- [16] J.H. Randrianalisoa, L.A. Dombrovsky, W. Lipiński, V. Timchenko. Effects of short-pulsed laser radiation on transient heating of superficial human tissues. *International Journal of Heat and Mass Transfer*, **78**: 488–497, 2014.
- [17] D. Fiala. *Dynamic Simulation of Human Heat Transfer and Thermal Comfort*. PhD Thesis, Institute of Energy and Sustainable Development De Montfort University Leicester, UK, 1998.
- [18] D. Fiala, G. Havenith, P. Bröde, B. Kampmann, G. Jendritzky. UTCI-Fiala multi-node model of human heat transfer and temperature regulation. *International Journal of Biometeorology*, **56**(3): 429–441, 2012.
- [19] A.A.A. Figueiredo, G. Guimarães. Estimation the intensity and location of a tumor using sequential function specification method. *Proceedings of CHT-15, ICHMT International Symposium on Advances in Computational Heat Transfer*, CHT-15-085, Rutgers University, USA, 2015.
- [20] A.P. Gagge. Rational temperature indices of man's thermal environment and their use with a 2-node model of his temperature regulation. *Fed. Proc.*, **32**: 1572–1582, 1973.

- [21] D. Gamerman, H.F. Lopes. *Markov Chain Monte Carlo: Stochastic Simulation for Bayesian Inference*, Chapman & Hall/CRC, 2nd edition, Boca Raton, 2006.
- [22] J. Geweke. Evaluating the Accuracy of Sampling-Based Approaches to the Calculation of Posterior Moments. [In:] *Bayesian Statistics*, J. Bernardo, J. Berger, A. Dawid, A. Smith [Eds.], Oxford University Press, 1992.
- [23] R.G. Gordon. *The Response of Human Thermoregulatory System in the Cold*. PhD Thesis (in Mechanical Engineering), University of California, Santa Barbara CA, 1974.
- [24] H. Haario, E. Saksman, J. Tamminen. An adaptive Metropolis algorithm. *Bernoulli*, **7**: 223–242, 2001.
- [25] J. Hadamard. *Lectures on Cauchy's Problem in Linear Differential Equations*. Yale University Press, New Haven, CT, 1923.
- [26] J.D. Hardy, J.A.J. Stolwijk. Partitional calorimetric studies of man during exposures to thermal transients. *J. Appl. Physiol.*, **21**: 1799–1806, 1966.
- [27] W.K. Hastings. Monte Carlo sampling methods using Markov chains and their applications. *Biometrika*, **57**: 97–109, 1970.
- [28] E. Hensel. *Inverse Theory and Applications for Engineers*. Prentice Hall, New Jersey, 1991.
- [29] K.R. Holmes. Native thermal conductivity of biomaterials (Appendix A) and the blood perfusion rates for special tissues and organs (Appendix B). [In:] *The CRC Handbook of Thermal Engineering Advances in Heat Transfer*, F. Kreith [Ed.], Springer Science & Business Media, 2000.
- [30] Ch-H. Huang, Ch-Y. Huang. An inverse problem in estimating simultaneously the effective thermal conductivity and volumetric heat capacity of biological tissue. *Applied Mathematical Modelling*, **31**: 1785–1797, 2007.
- [31] J. Kaipio, E. Somersalo. *Statistical and Computational Inverse Problems*, Applied Mathematical Sciences 160, Springer-Verlag, 2004.
- [32] J.P. Kaipio, C. Fox. The Bayesian framework for inverse problems in heat transfer. *Heat Transfer Engineering*, **32**(9): 718–753, 2011.
- [33] B. Kateb, V. Yamamoto, Ch. Yu, W. Grundfest, J.P. Gruen. Infrared thermal imaging: a review of the literature and case report. *NeuroImage*, **47**: T154–T162, 2009.
- [34] K. Kurpisz, A.J. Nowak. *Inverse Thermal Problems*. WIT Press, Southampton, UK, 1995.
- [35] P.M. Lee. *Bayesian Statistics*. Oxford University Press, London, 2004.
- [36] B. Lamien, H.R.B. Orlande, G. Elicabe, A. Maurente. State estimation problem in hyperthermia treatment of tumors loaded with nanoparticles. *Proc. of 15th Int. Heat Trans. Conf.*, IHTC15-8772: 1–14, 2014.
- [37] E. Majchrzak. *Modelling and analysis of thermal phenomena. Part IV. Mechanics. Technical Mechanics* [in Polish: *Modelowanie i analiza zjawisk termicznych. Część IV. Mechanika Techniczna*], Tom XII: Biomechanika, pod red. R. Będzińskiego, IPPT PAN, Warszawa, 223–361, 2011.
- [38] E. Majchrzak, B. Mochnacki. Sensitivity analysis and inverse problems in bio-heat transfer modeling. *Computer Assisted Mechanics and Engineering Sciences*, **13**(1): 85–108, 2006.
- [39] E. Majchrzak, M. Paruch. Identification of electromagnetic field parameters assuring the cancer destruction during hyperthermia treatment. *Inverse Problems in Science and Engineering*, **19**(1): 45–58, 2011.
- [40] MATLAB and Statistics Toolbox Release 2009b, The MathWorks, Inc., Natick, Massachusetts, United States, 2009.
- [41] N. Metropolis, A. Rosenbluth, M. Rosenbluth, A. Teller, E. Teller. Equation of state calculation by fast computing machines. *J. Chemical Phys.*, **21**: 1087–1092, 1953.
- [42] V.A. Morozov. *Methods for Solving Incorrectly Posed Problems*. Springer Verlag, New York, 1984.
- [43] D.A. Murio. *The Mollification Method and the Numerical Solution of Ill-Posed Problems*. Wiley Interscience, New York, 1993.
- [44] H.R.B. Orlande. Inverse problems in heat transfer: New trends on solution methodologies and applications. *Journal of Heat Transfer*, **134**: 031011, 2012.
- [45] H.R.B. Orlande, G.S. Dulikravich, M. Neumayer, D. Watzenig, M.J. Colaço. Accelerated Bayesian inference for the estimation of spatially varying heat flux in a heat conduction problem. *Numerical Heat Transfer Part A: Applications*, **65**: 1–25, 2014.
- [46] H.R.B. Orlande, F. Fudym, D. Mailet, R. Cotta. *Thermal Measurements and Inverse Techniques*. CRC Press, Boca Raton, 2011.
- [47] Z. Ostrowski, P. Buliński, W. Adamczyk, A.J. Nowak. Modelling and validation of transient heat transfer processes in human skin undergoing local cooling. *Przegląd Elektrotechniczny*, R. 91 NR 5/2015.
- [48] M.N. Ozisik, H.R.B. Orlande. *Inverse Heat Transfer: Fundamentals and Applications*. Taylor and Francis, New York, 2000.
- [49] K. Parsons. *Human Thermal Environments*. Taylor & Francis, 2003.
- [50] M. Paruch, E. Majchrzak. Identification of tumor region parameters using evolutionary algorithm and multiple reciprocity method. *Engineering Applications of Artificial Intelligence*, **20**(5): 647–655, 2007.
- [51] H.H. Pennes. Analysis of tissue and arterial blood temperatures in the resting human forearm. *Journal of Applied Physiology*, **1**(2): 93–122, 1948.
- [52] P.C. Sabatier. *Applied Inverse Problems*. Springer Verlag, Hamburg, 1978.
- [53] N. Severens. *Modelling hypothermia in patients undergoing surgery*. PhD Thesis, TU/e, Eindhoven, 2008.

- [54] N. Silver. *The Signal and the Noise*. Penguin Press, New York, 2012.
- [55] C.F.L. Souza, M.V.C. Souza, M.J. Colaço, A.B. Caldeira, F. Scofano Neto. Inverse determination of blood perfusion coefficient by using different deterministic and heuristic techniques. *J. Braz. Soc. Mech. Sci. Eng.*, **36**: 193–206, 2014.
- [56] S. Tan, C. Fox, G. Nicholls. Inverse Problems. *Course Notes for Physics 707*, University of Auckland, 2006.
- [57] A. Tarantola. *Inverse Problem Theory*. Elsevier, 1987.
- [58] A.N. Tikhonov, V.Y. Arsenin. *Solution of Ill-Posed Problems*. Winston & Sons, Washington, DC, 1977.
- [59] D.M. Trujillo, H.R. Busby. *Practical Inverse Analysis in Engineering*. CRC Press, Boca Raton, 1997.
- [60] V. Umadevi, S.V. Raghavan, S. Jaipurkar. Framework for estimating tumour parameters using thermal imaging. *Indian J. Med. Res.*, **134**: 725–731, 2011.
- [61] L.A.B. Varon, H.R.B. Orlande, G.E. Eliçabe. Estimation of state variables in the hyperthermia therapy of cancer with heating imposed by radiofrequency electromagnetic waves. *International Journal of Thermal Sciences*, **98**: 228–236, 2015.
- [62] C. Vogel. *Computational Methods for Inverse Problems*. SIAM, Philadelphia, 2002.
- [63] J. Werner, M. Buse. Temperature profiles with respect to inhomogeneity and geometry of the human body. *J. Appl. Physiol.*, **65**(3): 1110–1118, 1988.
- [64] R. Winkler. *An Introduction to Bayesian Inference and Decision*. Probabilistic Publishing, Gainesville, 2003.
- [65] E.H. Wissler. A mathematical model of the human thermal system. *Bulletin of Mathematical Biophysics*, **26**: 147–166, 1964.
- [66] E.H. Wissler. Pennes’ 1948 paper revisited. *Journal of Applied Physiology*, **85**: 35–41, 1998.
- [67] K. Woodbury. *Inverse Engineering Handbook*. CRC Press, Boca Raton, 2002.
- [68] P. Yuan, S-B. Wang, H-M. Lee. Estimation of the equivalent perfusion rate of Pennes model in an experimental bionic tissue without blood flow. *International Communications in Heat and Mass Transfer*, **39**: 236–241, 2012.
- [69] A.G. Yagola, I.V. Kochikov, G.M. Kuramshina, Y.A. Pentin. *Inverse Problems of Vibrational Spectroscopy*. VSP, Netherlands, 1999.